Implementation of Melt Eruption and Water Ingression Models in CINEMA for Molten Corium-Concrete Interaction Analysis

Chanyong Lee*, Seokwon Whang, Suwon Lee, Soonho Park, JinYong Lee
FNC Technology Co., Ltd., 32F, 13 Heungdeok 1-ro, Giheung-gu, Yongin-si, Gyeonggi-do, 16954, Republic of Korea
**Corresponding author: coldragon@fnctech.com*

***Keywords : CINEMA, SACAP, MCCI, Melt eruption, Water ingression**

1. Introduction

During a severe accident, progression of core degradation and subsequent reactor pressure vessel failure may result in the relocation of high temperature corium to the concrete basemat of the reactor cavity. Upon contact with the concrete, molten corium-concrete interaction (MCCI) is initiated, involving coupled thermal and chemical processes between the corium and concrete. Continued MCCI leads to concrete decomposition and ablation driven by heat transfer from the molten pool. In addition, the release of free and chemically bound water generates steam and carbon dioxide, with the decomposition of carbonate phases in the concrete. These gases can affect convective heat transfer and oxidation reactions within the melt pool, while also contributing to containment pressurization. In the absence of adequate long-term cooling, sustained basemat ablation may challenge the structural integrity of the containment and potentially compromise its confinement function. Therefore, the development of MCCI analysis models capable of predicting melted corium temperature, concrete ablation, and corium coolability has remained an important research topic for assessing ex-vessel severe accident progression and containment integrity.

CINEMA (Code for INtegrated severe accident Evaluation and MAnagement) is an integrated severe accident analysis code developed in Korea to simulate the overall progression of a severe accident, from accident initiation and core degradation to reactor pressure vessel (RPV) failure, ex-vessel corium behavior, and fission-product behavior. CINEMA consists of CSPACE (Core meltdown progress simulation coupling with Safety and Performance Analysis CodE for nuclear power plants) for in-vessel phenomena, SIRIUS (Simulation of Radioactive nuclide Interaction Under Severe accident) for fission-product behavior, SACAP (Severe Accident Containment Analysis Package) for ex-vessel phenomena, and MASTER for the integrate of calculation data among the modules. CSPACE simulates the thermal-hydraulic behavior of the reactor coolant system, core degradation, and RPV failure, whereas SIRIUS calculates the release, transport, and aerosol behavior of fission products. MASTER manages the coupled calculation, including the exchange of mass and thermal hydraulic data between CSPACE, SIRIUS, and SACAP.

SACAP (Severe Accident Containment Analysis Package) simulates ex-vessel severe-accident phenomena occurring in the containment following RPV failure. The containment is represented by a network of control volumes and junctions, enabling calculation of containment pressure, temperature, gas composition, and coolant behavior. Major severe-accident phenomena, including hydrogen combustion, fuel–coolant interaction (FCI), high-pressure melt ejection/direct containment heating (HPME/DCH), and MCCI, are considered.

In the present study, melt eruption and water ingression models were incorporated into SACAP to simulate top flooding coolability during MCCI. Water ingression refers to the penetration of overlying water through cracks in the crust, providing additional heat removal from the underlying melt. Melt eruption refers to the entrainment of molten corium by concrete-decomposition gases into the overlying water, where a particle debris bed may subsequently form. Both mechanisms enhance heat transfer to the overlying water and can mitigate corium cooling time and concrete ablation. The model performance was assessed against the OECD/MCCI CCI-2 and CCI-3 experiments [1], which differ in concrete composition and directional ablation characteristics, using measured melt temperatures, water layer heat fluxes, and concrete ablation depths.

2. Methodology

Melt eruption refers to the entrainment of molten corium by concrete decomposition gases as they pass through cracks in the upper crust and enter the overlying water. The erupted melt can form the particle debris bed in the water, increasing the effective heat-transfer area and promoting melt-pool cooling and mitigating concrete ablation. The melt superficial velocity induced by melt eruption was calculated using the Ricou-Spalding entrainment correlation [3]:

$$j_m = K_e j_g$$

$$K_e = E\left(\frac{\rho_g}{\rho_m}\right)^{\frac{1}{2}}$$

where j_m and j_g are the superficial velocities of the melt and gas, respectively. Also, Ke, E, ρ_g, and ρ_m refers to the entrainment coefficient, model constant, gas density, and melt density, respectively. The calculated erupted melt was added to the mass of the particle bed, while the corresponding mass and enthalpy were

removed from the melt pool to ensure mass and energy conservation.

Under top flooding conditions, the crust formed at the melt surface may crack owing to thermal stresses. Water ingression is defined as the penetration of overlying water through these cracks into the crust, thereby enhancing heat removal from the underlying melt. In this study, a crust dryout heatflux correlation proposed by Lister-Epstein [2] was adopted. Water ingression into the crust was assumed to occur when the top-surface heat flux of the crust, (q''_{top}), was lower than the dryout heat flux, (q''_{dry}):

$$q''_{top} < q''_{dry}$$

The dryout heat flux was calculated as a function of crust thermal properties, coolant and vapor properties, the thermal-expansion coefficient, and the cracking temperature:

$$q''_{dry} = C_{dry} \left\{ \left[\left(\frac{h_{lv}(\rho_l - \rho_v)g}{\nu_v} \right)^5 \left[\frac{N_{dry} k_c^2 (\Delta e_{sat})^2}{c_p \Delta e_{cr}} \right]^4 \right] \right\}^{\frac{1}{13}} \times [\alpha_T (T_{cr} - T_{sat})]^{\frac{15}{13}}$$

where, C_{dry} is an empirical constant, k_c is the crust thermal conductivity, α_T is the thermal-expansion coefficient, and T_{cr} and T_{sat} are the cracking and coolant saturation temperatures, respectively. The additional heat removal induced by water ingression was incorporated as enhanced heat transfer to the overlying water, thereby reducing the heat flux transferred from the melt pool to the melt-concrete interface and the concrete ablation rate.

To assess the effects of the implemented models, simulations were performed for the CCI-2 and CCI-3 tests conducted under the OECD/MCCI program. These large-scale, two-dimensional MCCI tests were initially conducted under dry-cavity conditions and subsequently subjected to top flooding to investigate corium coolability and concrete ablation behavior. Although both tests employed the same test-section geometry, CCI-2 used limestone/common-sand (LCS) concrete, whereas CCI-3 used siliceous concrete. The tests therefore provide data for assessing MCCI behavior under different concrete compositions and decomposition-gas characteristics. Melt temperature, concrete ablation depth, and heat flux to the overlying water layer were measured.

Within SACAP, heat transfer from a molten corium layer to the concrete is evaluated using a modified Kutateladze-Malenkov correlation coupled with a Bradley slag-film resistance. The correlation represents convection enhancement by concrete decomposition gases, whereas the slag film is treated as an additional thermal resistance in series with the melt-side convective resistance:

$$q''_c = h_{eff}(T_m - T_{abl})$$

$$h_{eff} = \left(\frac{1}{h_{KM}} + \frac{1}{h_{slag}} \right)^{-1}, \quad h_{slag} = C_{slag}\, h_{KM}$$

$$h_{KM} = \frac{k_m}{r_b} \left[1.5 \cdot 10^{-3} K_u^{\frac{2}{3}} f(w) \right]$$

where h_{eff}, h_{KM}, and h_{slag} are the effective, corium convective, and slag film convective heat transfer coefficients, respectively. C_{slag} is the Bradley slag-film factor. K_u is the Kutateladze number, r_b is the bubble radius, and w is the dimensionless gas velocity.

Accordingly, this correlation was applied to the CCI-2 simulation to estimate and validate temperature and ablation depth to experiments. For CCI-3, however, the basemat and sidewall heat-transfer coefficients were specified using the empirical correlations proposed by Sevón [4] to represent the observed anisotropic ablation. The test matrix is summarized in Table 1.

Table 1. Test matrix and specifications of CCI tests

Parameter	CCI-2	CCI-3
Geometry (cm x cm)	50 x 50	
Concrete Type	Limestone/ Common Sand	Siliceous
Initial Mass (kg)	400	375
Water Adding Time (sec)	18000	6300
Decay Heat (kW)	120	
Water Flow Rate (L/s)	2	
Total Test Time (sec)	25600	10800

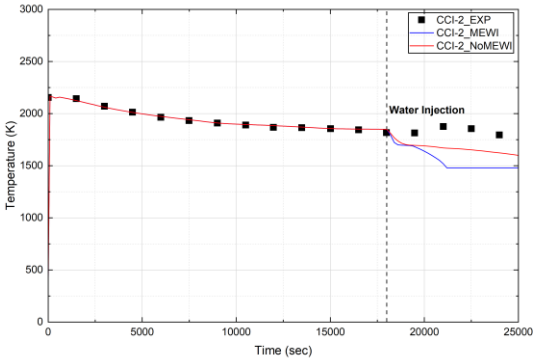
3. Results and Discussion

Fig. 1 compares the measured melt temperatures in the CCI-2 and CCI-3 tests with SACAP calculations performed with and without the melt eruption and water ingression models.

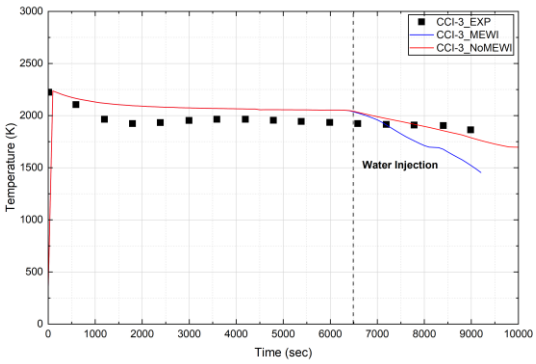
In Fig. 1(a) for CCI-2 tests, the simulated temperature decrease before cavity flooding at 18,000 s generally follows the measured trend, with a discrepancy of approximately 30 K at the flooding time. At the beginning of the calculation, however, the predicted temperature decreases more rapidly than the measured temperature. This difference appears to be associated with the onset of concrete ablation, whereas ablation begins at approximately 2,000 s in the experiment. The calculated melt temperature is already above the ablation temperature, resulting in immediate ablation. After flooding, the calculation with melt eruption and water ingression predicts a sharp temperature reduction. Although this behavior indicates a strong cooling effect of the two mechanisms, the calculated temperature trend differs from the measurement. Therefore, additional assessments will be conducted on the empirical parameters used in the two models.

In Fig. 1(b) for CCI-3 tests, the simulated temperature discrepancy is approximately 114 K before water addition at 6,300 s. In contrast to CCI-2, the calculated temperature trend during the dry cavity phase agrees relatively less with the measurement. This behavior is

likely related to the lower axial convective heat transfer coefficient of 100 W/m2-K, which slows axial ablation and affects heat transfer. As in CCI-2, the calculation including melt eruption and water ingression shows a pronounced effect of the coolability mechanisms after flooding.



(a) CCI-2 Result

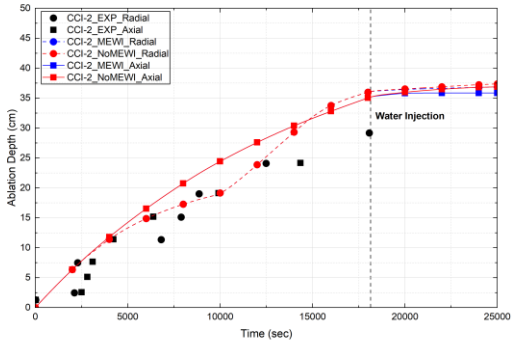


(b) CCI-3 Result

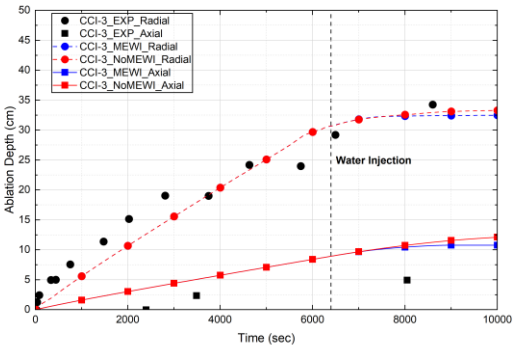
Figure 1. Comparison of measured and calculated melt temperatures in the CCI tests.

Fig. 2 compares the measured and calculated concrete ablation depths in the CCI tests. In Fig. 2(a), the measured axial and lateral ablation depths of CCI-2 are comparable, whereas the calculated results differ by approximately 5 cm. Nevertheless, the calculation reproduces the approximately uniform ablation observed experimentally in the both directions. In the simulation including melt eruption and water ingression, concrete ablation ceases after water addition, demonstrating the cooling effect of the implemented models. In contrast, ablation continues after water injection in the calculation without the melt eruption and water ingression models.

In Fig. 2(b), the measured lateral ablation of CCI-3 is greater than the axial ablation, unlike the CCI-2 result. The calculated lateral ablation depth is close to the measurement, while the axial ablation depth differs by approximately 5 cm. The origin of this asymmetric ablation behavior remains uncertain. One possible explanation reported for CCI-3 is that an insulating corium crust formed during the initial approximately 50 min of contact with cold concrete protected the basemat, while the sidewalls ablated immediately [4].



(a) CCI-2 Result

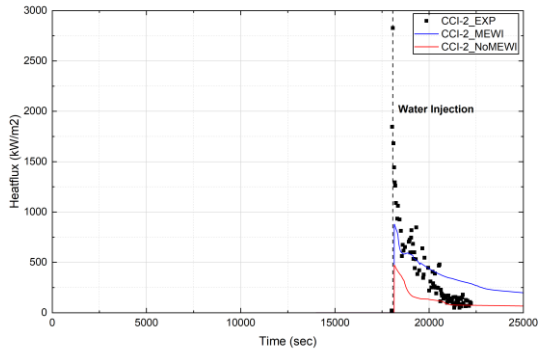


(b) CCI-3 Result

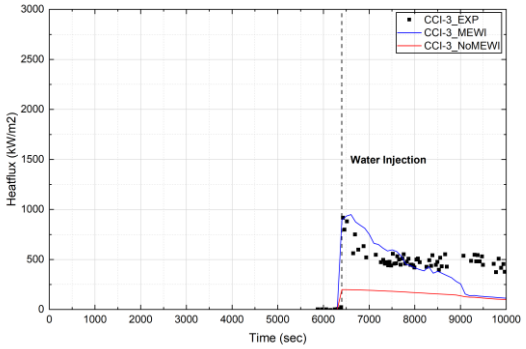
Figure 2. Comparison of measured and calculated axial and lateral concrete ablation depths in the CCI tests.

Fig. 3 compares the measured and calculated heat fluxes to the overlying water layer in the CCI tests. In both tests, the measured heat flux increases sharply immediately after water addition and then decreases continuously. The initial high heat flux is attributed to subcooled boiling when water is first injected. The heat flux subsequently decreases, and the calculation incorporating melt eruption and water ingression more closely reproduces the measured trend.

The calculated heat flux with improved models predicts a marked increase in heat transfer to the overlying water. This result indicates that both models enhance heat removal through the otherwise limiting crust heat transfer path.



(a) CCI-2 Result



(b) CCI-3 Result

Figure 3. Comparison of measured and calculated heat fluxes to the overlying water layer in the CCI tests.

4. Conclusion

In this study, melt eruption and water ingression models were incorporated into the SACAP model, and their applicability was assessed using the OECD/MCCI CCI-2 and CCI-3 tests. The models represent corium cooling and heat removal behavior following top flooding and enable the effects of concrete type on heat flux and concrete ablation to be examined.

Further quantitative comparisons with other computational code will be performed to quantify model prediction errors and identify directions for improvement.

5. Acknowledgement

This work was supported by Korea Hydro & Nuclear Power Co., Ltd. through the CINEMA code development project (No. L25S048000)

REFERENCES

[1] M. T. Farmer, S. Lomperski, D. J. Kilsdonk, R. W. Aeschlimann, and S. Basu, “OECD MCCI project final report, February 28, 2006.,” OECD/MCCI-2005-TR06, 1014859, May 2011. doi: 10.2172/1014859.

[2] M. Epstein, “Dryout Heat Flux During Penetration of Water Into Solidifying Rock,” *Journal of Heat Transfer*, vol. 128, no. 8, pp. 847–850, Aug. 2006, doi: 10.1115/1.2227042.

[3] M. T. Farmer, “The CORQUENCH Code for Modeling of Ex-Vessel Corium Coolability under Top FLooding Conditions,” ANL--18/22, 1483840, Aug. 2018. doi: 10.2172/1483840.

[4] T. Sevón, “A heat transfer analysis of the CCI experiments 1–3,” *Nuclear Engineering and Design*, vol. 238, no. 9, pp. 2377–2386, Sep. 2008, doi: 10.1016/j.nucengdes.2008.02.002.